ISBN: 978-3-95450-227-1 ISSN: 2673-5490 doi:10.18429/JACoW-IPAC2022-WEPOMS008

IMPACT OF BROADBAND IMPEDANCE ON LONGITUDINAL COUPLED-BUNCH INSTABILITY THRESHOLD*

I. Karpov† and E. Shaposhnikova, CERN, Geneva 23, Switzerland

Abstract

Coupled-bunch instabilities (CBI) and the loss of Landau damping (LLD) in the longitudinal plane can affect the performance of high-current synchrotrons. The former is driven by the narrowband impedance of resonant structures, while the latter is mainly determined by the broadband impedance of the entire accelerator and is a single-bunch effect. Therefore, the CBI and LLD thresholds are usually evaluated separately in order to define the corresponding critical impedance budget for given beam parameters. In this paper, we show that the CBI threshold in the presence of broadband impedance can be significantly lower than the one defined by only the narrowband impedance, especially if the LLD threshold is below the CBI threshold. In some cases, the beam becomes unstable even below the LLD threshold. This explains the low CBI threshold observed for the LHC-type beams in the CERN SPS. For HL-LHC, the broadband impedance may also significantly reduce the CBI threshold driven by higher-order modes of the crab cavities.

INTRODUCTION

A long-range wake-field induced by a beam due to a narrowband (NB) impedance in the ring may couple several bunches and, eventually, drive a coupled-bunch instability (CBI). This happens above a threshold beam intensity, which depends on beam and accelerator parameters. In absence of the synchrotron frequency spread inside the bunch (linear RF field) or other damping mechanisms (like synchrotron radiation damping) the threshold is zero. For this case, the growth rates of longitudinal CBI were first found by Sacherer [1] and analysed using different approaches (e.g. [2]).

For operation above the threshold intensity, a dedicated feedback system is required to keep the beam stable. Therefore the first mitigation step is usually to try and reduce (damp) the NB impedance below the critical (threshold) value. In the case of higher-order modes (HOM) in the RF resonators or other cavity-like structures, special couplers need to be designed and installed. This explains why the knowledge of the exact instability thresholds plays an important role, especially for the proton beams.

The CBI threshold can be accurately calculated using the approach developed in [3] and is based on solutions of the matrix equation derived by Lebedev [4] from the Vlasov equation. This matrix equation was also used recently, together with the method [5] suggested for analysis of single-bunch instability, to find the LLD threshold due to reactive impedance [6]. In particular, it was demonstrated that above transition energy, the threshold depends on the roll-off frequency of the inductive impedance, and it is zero for the constant $\mathrm{Im}Z/k$.

It is known that above the LLD threshold, a resistive component of the NB impedance can lead to CBI. For example, the CBI growth rates were affected when the broadband (BB) impedance was included in calculations [7]. Also, the growth rates of CBI driven by the low-frequency NB impedance in the presence of space charge impedance (without truncation in frequency) were recently derived [8]. In this paper, we use the Lebedev matrix equation to evaluate the CBI threshold taking into account two types of impedance sources. Then we present the results of self-consistent semi-analytical calculations with the code MELODY [9] and compare them with macro-particle tracking simulations using the code BLonD [10].

INSTABILITY THRESHOLD

The Lebedev equation [4] can be applied to evaluate beam stability for both single- and multi-bunch configurations. For the ring uniformly filled with L bunches it has a form

$$\tilde{\lambda}^l_{k'}(\Omega) = -\frac{\zeta}{h}\sum_{k=-\infty}^{\infty} G_{k'k}(\Omega)\,\frac{Z_k(\Omega)/k}{Z_0}\,\tilde{\lambda}^l_k(\Omega), \quad (1)$$

where $\tilde{\lambda}^l_k(\Omega)$ are the harmonics of the line-density perturbation for the frequency Ω with the coupled-bunch mode number l ($l = 0, 1, ..., L-1$), $k = f/f_0$, and $f_0 = \omega_0/(2\pi)$ is the revolution frequency, $Z_k(\Omega) = Z(k\omega_0 + \Omega)$ is the longitudinal impedance at frequency $k\omega_0 + \Omega$, and $Z_0 \approx 377\ \Omega$ is the impedance of free space. Note that $\tilde{\lambda}^l_k$ are non-zero only for $k = pL + l$, where $p = 0, \pm1, \pm2...$ We also introduced the dimensionless "intensity" parameter

$$\zeta = -\frac{qN_p\,h^2\,\omega_0\,Z_0}{V_0\cos\phi_{s0}}, \quad (2)$$

where q is the electrical charge, N_p is the number of particles per bunch, h is the harmonic number, V_0 is the RF voltage amplitude, and ϕ_{s0} is the synchronous phase.

The beam-transfer matrix elements $G_{k'k}$ in Eq. (1) are

$$G_{k'k}(\Omega) = -i\omega_{s0}^2\sum_{m=-\infty}^{\infty} m\int_0^{\mathcal{E}_{\max}}\frac{d\mathcal{F}(\mathcal{E})}{d\mathcal{E}}\,\frac{I_{mk}(\mathcal{E})I^*_{mk'}(\mathcal{E})}{\Omega - m\omega_s(\mathcal{E})}d\mathcal{E}, \quad (3)$$

with $f_{s0} = \omega_{s0}/2\pi$ being the frequency of small-amplitude synchrotron oscillations in a bare single-RF system, and

$$I_{mk}(\mathcal{E}) = \frac{1}{\pi}\int_0^{\pi} e^{i\frac{k}{h}\phi(\mathcal{E},\psi)}\cos m\psi\,d\psi, \quad (4)$$

* Work supported by the High Luminosity LHC project.
† ivan.karpov@cern.ch

ISBN: 978-3-95450-227-1 ISSN: 2673-5490 doi:10.18429/JACoW-IPAC2022-WEPOMS008

where m is the azimuthal mode number, $\mathcal{E}$ and ψ are the energy and phase of the synchrotron oscillations, respectively. In this work, we consider a stationary distribution function of the binomial family $\mathcal{F}(\mathcal{E}) \propto (1-\mathcal{E}/\mathcal{E}_{\max})^{\mu}$, where $\mathcal{E}_{\max}$ is the maximum energy of the synchrotron oscillations, and μ defines the bunch shape ($\mu \to \infty$ for Gaussian bunches).

Narrowband impedance

Let us consider first the CBI driven by a single resonator-impedance source

$$Z_{k,\mathrm{res}}(R,Q,f_r) = \frac{R}{1+iQ\left(\frac{kf_0}{f_r}-\frac{f_r}{kf_0}\right)}, \tag{5}$$

where R is the shunt impedance, Q is the quality factor, and f_r is the resonant frequency. If for the resonator bandwidth $\Delta f = \frac{f_r}{2Q}$, the following conditions are satisfied

$$\Delta f \ll L f_0, \text{ and } \Delta f \ll \left| f_r - \frac{pLf_0}{2} \right|, \tag{6}$$

all elements in Eq. (1) can be neglected except with $k_r = \lfloor f_r/f_0 \rfloor$, where $\lfloor x \rfloor$ denotes the rounding of x to the nearest integer. Thus, the instability threshold $\zeta_{\mathrm{th,NB}}$ can be found by solving the integral equation ($\mathrm{Im}\Omega \to +0$, $\mathrm{Re}\Omega = m\omega_s(\tilde{\mathcal{E}}_m)$, $0 < \tilde{\mathcal{E}}_m < \mathcal{E}_{\max}$)

$$\zeta_{\mathrm{th,NB}} = -h\left[G_{k_r k_r}(\Omega)\,\frac{Z_{k_r,\mathrm{res}}(\Omega)/k_r}{Z_0}\right]^{-1}, \tag{7}$$

and for some specific particle distributions, the analytic expression can be obtained [3, 11]. The threshold is mostly defined by the value of R/k_r, since the imaginary part of the resonator impedance around f_r is close to zero.

Narrowband and broadband impedances

For the sake of simplicity, we will consider here a combination of NB impedance and the reactive impedance truncated at the frequency f_c: $\mathrm{Im}Z_{k,\mathrm{reac}}/k = \text{const}$ for $|k| < k_c = f_c/f_0$, and 0 elsewhere. Other BB impedance sources can be treated similarly. The solution of Eq. (1) exists for Ω if the following determinant

$$\begin{aligned}&\det\left|\delta_{k'k} + \frac{\zeta}{h}\,G_{k'k}(\Omega)\frac{Z_k(\Omega)/k}{Z_0}\right| \\ &\approx 1 + \frac{\zeta}{h}\sum_{k=-\infty}^{\infty} G_{kk}(\Omega)\,\frac{Z_k(\Omega)/k}{Z_0}\end{aligned} \tag{8}$$

equals zero. Similarly to [6], we used the matrix property:

$$\det\left[\exp\left(\varepsilon\, X\right)\right] = \exp\left[\varepsilon\,\mathrm{tr}\left(X\right)\right],$$

where $\mathrm{tr}(X)$ is the trace of an arbitrary square matrix X, and $\varepsilon \ll 1$ is some small parameter. Thus, the instability threshold for this more general case

$$\begin{aligned}\zeta_{\mathrm{th}} \approx -h\Bigg[&G_{k_r k_r}(\Omega)\,\frac{Z_{k_r,\mathrm{res}}(\Omega)/k_r}{Z_0} \\ &-\frac{\mathrm{Im}Z_{k,\mathrm{reac}}/k}{Z_0}\sum_{|k|\le k_c}\mathrm{Im}G_{kk}(\Omega)\Bigg]^{-1}.\end{aligned} \tag{9}$$

Even if the $\mathrm{Im}Z_{k,\mathrm{reac}}/k$ is smaller than R/k_r, the contribution from the inductive impedance can still be significant due to the sum over k, since G_{kk} is a symmetric and rather smooth function of k. The CBI threshold ζ_{th} (9) can differ significantly from the one defined in Eq. (7) by the NB impedance only and will be lower than the LLD threshold (see examples below). Note that, if we neglect the term with reactive impedance in Eq. (9), the threshold becomes identical to Eq. (7). On the other hand, neglecting the NB impedance and performing the sum for $k = \pm 1, \pm 2, \ldots \pm k_c$, we recover the expression for the LLD threshold [6].

INSTABILITY FOR UNIFORM FILLING

In this section, we present the results of semi-analytical calculations for the LHC at the injection energy with parameters summarised in Table 1. To reach the target luminosity with the nominal HL-LHC bunch intensity ($N_p = 2.3\times10^{11}$), two types of crab cavities, Double Quarter Wave (DQW) [12] and RF-Dipole (RFD) [13], will be installed in the LHC. The HOM of the DQW crab cavity ($R = 71$ kΩ, $f_r \approx 582$ MHz, and $Q = 1360$ [12]) has the lowest CBI threshold based on calculations neglecting BB impedance. Thus, its threshold is evaluated here by taking into account the full accelerator impedance. Since the detailed LHC impedance model is still under development, we will use a BB resonator impedance with $Q = 1$, $f_r = 5$ GHz, and $R = 38$ kΩ (the assumption is based on the concept of the effective impedance [6, 14]).

A new version of the code MELODY was developed for semi-analytical studies of the CBI for arbitrary impedance models. In particular, the Oide-Yokoya method [5] was extended to compute separately the eigenvalues of the corresponding coupled-bunch mode l. We assume a uniformly filled ring with bunches spaced by ten RF buckets ($L = 3564$) and consider the worst-case scenario for which the HOM frequencies of all four crab cavities overlap.

An example of the computed CBI growth rate as a function of the single-bunch intensity is shown in Fig. 1. The CBI threshold is reduced by almost a factor of three when the BB impedance is included, compared to the one defined by the HOM of crab cavities only, as predicted by Eq. (9). Moreover, the instability threshold is very close to the LLD threshold (dashed line) and, thus, dominated by the inductive part of the BB impedance. This is why the precise BB

Table 1: The accelerator and RF parameters of the SPS and the LHC at 450 GeV beam energy [15].

Parameter	Units	SPS	LHC
Circumference, C	m	6911.55	26658.86
Harmonic number, h		4620	35640
Transition gamma, γ_{tr}		17.95	55.76
RF frequency, f_{RF}	MHz	200.39	400.79
RF voltage, V_0	MV	7.2	8

ISBN: 978-3-95450-227-1 ISSN: 2673-5490 doi:10.18429/JACoW-IPAC2022-WEPOMS008

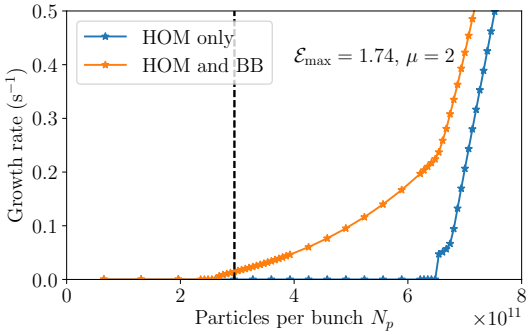

Figure 1: The growth rate of multi-bunch instabilities in the LHC as a function of bunch intensity for HOM impedance with (orange) and without (blue) BB impedance. The vertical line corresponds to the LLD threshold. Beam and accelerator parameters are detailed in Table 1.

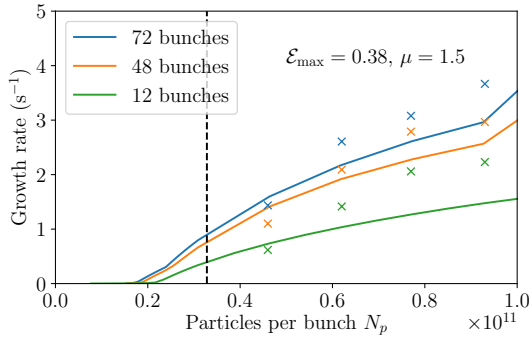

Figure 2: The growth rate of multi-bunch instabilities in the SPS as a function of bunch intensity for different numbers of bunches in the train. The vertical line corresponds to the LLD threshold. The crosses indicate the fitted growth rate from macroparticle simulations with BLonD. Beam and accelerator parameters are from Table 1.

impedance model is necessary to make accurate predictions of the CBI threshold for the HL-LHC parameters. The detailed analysis of the mode structure shows that above the CBI threshold with BB impedance, the line-density perturbation is localised in the bunch centre as for the case of single-bunch LLD. On the contrary, in the absence of BB impedance, the perturbation involves mainly high-amplitude particles.

INSTABILITY OF BUNCH TRAINS

In this section, we show the results for the LHC-type beam in the SPS. The code MELODY was further extended to evaluate beam stability for a partial (arbitrary) filling pattern as in the SPS. The total matrix includes the contributions from all bunches individually and all possible modes are computed simultaneously. The detailed SPS impedance model [16] and one-turn delay feedback model [17, 18] for the 200 MHz RF system were used for the analysis presented below. The results of calculations with MELODY for the SPS parameters at the extraction energy (Table 1) for different numbers of bunches used in operation are shown in Fig. 2. As expected, the threshold of instability weakly depends on the number of bunches due to a strong impact of the BB impedance of the SPS and it is significantly lower than the threshold defined by any HOM impedance. For example, for the HOM of the 200 MHz RF cavities around 630 MHz, it is about 6×10^{11} for 12 bunches. Above the threshold, the growth rates are larger for a longer train as the instability builds up along the bunches. Note that the instability threshold is again below the LLD threshold (dashed line).

Finally, the semi-analytical predictions were compared with the simulation results obtained using the code BLonD [10]. The CBI of the dipole mode has the lowest threshold in this case and manifests through the oscillations of the bunch position. The MELODY predictions agree well with the BLonD results (Figs. 2,3). Some differences can be explained by the fact that several coupled-bunch modes are excited at the same time which can interfere and modify the bunch position oscillations.

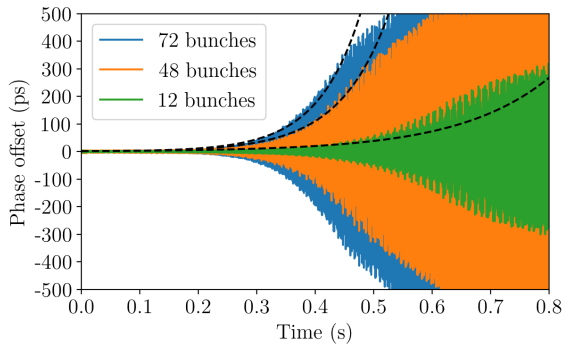

Figure 3: Time evolution of bunch position from BLonD simulations for different numbers of bunches in a train with $N_p = 6.2 \times 10^{10}$. The black dashed curve shows the expected increase of oscillation amplitudes based on the growth rate of the most unstable mode found with MELODY. All parameters are as in Fig. 2.

CONCLUSION

In the present work, we have shown that the broadband impedance of the accelerator can significantly reduce the threshold of coupled-bunch instability driven by the narrow-band impedance. The general expression for the multi-bunch instability threshold in the presence of two different types of impedance has been derived using the Lebedev matrix equation. For LHC and the LHC-type beams in the SPS, we have found that the instability threshold is even lower than the threshold of loss of Landau damping. For the bunch trains in the SPS, the results are consistent with the experimental observations and also agree with macroparticle simulations. We have demonstrated that an accurate broadband impedance model is essential for reliable prediction of multi-bunch instability thresholds.

ACKNOWLEDGEMENTS

We are grateful to H. Damerau for useful comments.

ISBN: 978-3-95450-227-1 ISSN: 2673-5490 doi:10.18429/JACoW-IPAC2022-WEPOMS008

REFERENCES

[1] F. J. Sacherer, "A longitudinal stability criterion for bunched beams," *IEEE Transactions on Nuclear Science*, vol. 20, no. 3, pp. 825–829, 1973, doi:10.1109/TNS.1973.4327254

[2] J. L. Laclare, "Bunched beam coherent instabilities," CERN, Tech. Rep. CERN-1987-003-V-1.264, 1987, doi:10.5170/CERN-1987-003-V-1.264

[3] V. I. Balbekov and S. V. Ivanov, "Longitudinal beam instability threshold beam in proton synchrotrons," *Atomic Energy*, vol. 60, no. 1, pp. 58–66, 1986, doi:10.1007/BF01129839

[4] A. N. Lebedev, "Coherent synchrotron oscillations in the presence of a space charge," *Atomic Energy*, vol. 25, no. 2, pp. 851–856, 1968, doi:10.1007/BF01121037

[5] K. Oide and K. Yokoya, "Longitudinal single bunch instability in electron storage rings," KEK, Tech. Rep. KEK-Preprint-90-10, 1990.

[6] I. Karpov, T. Argyropoulos, and E. Shaposhnikova, "Thresholds for loss of landau damping in longitudinal plane," *Phys. Rev. Accel. Beams*, vol. 24, p. 011 002, 1 2021, doi:10.1103/PhysRevAccelBeams.24.011002

[7] M. Blaskiewicz, "Longitudinal Stability Calculations," BNL, Tech. Rep. BNL-81969-2009-IR, 2009.

[8] A. Burov, "Longitudinal modes of bunched beams with weak space charge," *Phys. Rev. Accel. Beams*, vol. 24, p. 064 401, 6 2021, doi:10.1103/PhysRevAccelBeams.24.064401

[9] I. Karpov, Matrix Equations for LOngitudinal beam DYnamics (MELODY) code, https://gitlab.cern.ch/ikarpov/melody.

[10] CERN Beam Longitudinal Dynamics code BLonD, http://blond.web.cern.ch.

[11] I. Karpov and E. Shaposhnikova, "Longitudinal Coupled-Bunch Instability Evaluation for FCC-hh," in *Proc. 10th International Particle Accelerator Conference (IPAC'19), Melbourne, Australia, 19-24 May 2019*, 2019, pp. 297–300, doi:doi:10.18429/JACoW-IPAC2019-MOPGW083

[12] J. Mitchell, G. Burt, R. Calaga, S. Verdú-Andrés, and B. P. Xiao, "DQW HOM Coupler Design for the HL-LHC," in *Proc. 9th International Particle Accelerator Conference (IPAC'18), Vancouver, BC, Canada, April 29-May 4, 2018*, Vancouver, BC, Canada, 2018, pp. 3663–3666, doi:doi:10.18429/JACoW-IPAC2018-THPAL018

[13] S. D. Silva, P. Berrutti, J. Delayen, N. Huque, and H. Park, "Room Temperature Measurements of Higher Order Modes for the SPS Prototype RF-Dipole Crabbing Cavity," in *Proc. 9th International Particle Accelerator Conference (IPAC'18), Vancouver, BC, Canada, April 29-May 4, 2018*, Vancouver, BC, Canada, 2018, pp. 3805–3807, doi:doi:10.18429/JACoW-IPAC2018-THPAL067

[14] I. Karpov, T. Argyropoulos, S. Nese, and E. Shaposhnikova, "New Analytical Criteria for Loss of Landau Damping in Longitudinal Plane," in *Proc. HB'21*, Batavia, IL, USA, 2022, paper MOP16, pp. 100–105, doi:10.18429/JACoW-HB2021-MOP16

[15] O. Brüning *et al.*, "LHC design report vol.1: The LHC main ring," CERN, Tech. Rep. CERN-2004-003-V-1, 2004, doi:10.5170/CERN-2004-003-V-1

[16] CERN SPS Longitudinal Impedance Model, https://gitlab.cern.ch/longitudinal-impedance/SPS.

[17] F. J. Galindo Guarch, P. Baudrenghien, and J. M. Moreno Arostegui, "A new beam synchronous processing architecture with a fixed frequency processing clock. application to transient beam loading compensation in the cern sps machine," *Nuclear Instruments and Methods in Physics Research Section A: Accelerators, Spectrometers, Detectors and Associated Equipment*, vol. 988, p. 164 894, 2021, doi:https://doi.org/10.1016/j.nima.2020.164894

[18] One Turn Delay Feedback static model, https://gitlab.cern.ch/ikarpov/sps_otfb_static_model.